

## Supporting Information

### **Thirty-minute preparation of microporous polyimides with high surface area for ammonia adsorption**

Tingting Zhu,<sup>a†</sup> Baoyou Pei,<sup>b†</sup> Tuo Di,<sup>a</sup> Yunxia Xia,<sup>a</sup> Tiesheng Li<sup>c</sup> and Lei Li<sup>\*a</sup>

a College of Materials and Fujian Provincial Key Laboratory of Materials Genome, Xiamen University, Xiamen, 361005, P.R. China

b Department of Materials Science and Engineering, Huaqiao University, Xiamen, 361021, P.R. China

c College of Chemistry and Molecular Engineering, Zhengzhou University, Zhengzhou, 450001, P.R. China

† Tingting Zhu and Baoyou Pei contributed equally to this work.

E-mail: lilei@xmu.edu.cn

Tel: +86-592-2186296

Fax: +86-592-2183937

Table S1. Polymerization conditions for the preparation of MPIs.

Samples	Triamines			NCDH (g)	DPS (g)	Polymerization conditions
	TAPA (g)	TAPT (g)	TAPB (g)			
MPI-A-30	0.0581	-	-	0.0805	0.2772	325 °C, 0.5 h
MPI-T-30	-	0.0709	-	0.0805	0.3028	325 °C, 0.5 h
MPI-B-30	-	-	0.0703	0.0805	0.3016	325 °C, 0.5 h
MPI-A-60	0.0581	-	-	0.0805	0.2772	325 °C, 1.0 h
MPI-A-90	0.0581	-	-	0.0805	0.2772	325 °C, 1.5 h
MPI-A-30-1	0.1452	-	-	0.2011	0.6926	325 °C, 0.5 h
MPI-A-30-2	0.1161	-	-	0.1609	0.5540	325 °C, 0.5 h
MPI-A-30-3	0.0871	-	-	0.1207	0.4156	325 °C, 0.5 h
MPI-A-30-4	0.0581	-	-	0.0805	0.2772	325 °C, 0.5 h

Table S2. Elemental analysis of MPIs

Samples	Experimental (wt%)				Theoretical (wt%)			
	C	H	N	S	C	H	N	S
<b>MPI-A-30</b>	68.45	3.84	8.48	1.20	73.35	2.84	8.77	0
<b>MPI-T-30</b>	66.08	3.44	11.01	1.51	71.79	2.56	11.97	0
<b>MPI-B-30</b>	72.35	3.27	5.69	0.85	77.25	3.00	6.00	0

Table S3. Elemental analysis of pure DPS and recovered DPS.

Samples	Experimental (wt%)				Theoretical (wt%)			
	C	H	N	S	C	H	N	S
<b>DPS</b>	65.02	4.39	0.29	15.52	66.06	4.59	0	14.68
<b>DPS-1</b>	65.00	4.18	0.31	14.84	-	-	-	-
<b>DPS-2</b>	64.92	4.43	0.34	14.85	-	-	-	-
<b>DPS-3</b>	64.91	4.34	0.36	14.71	-	-	-	-
<b>DPS-4</b>	65.12	4.54	0.28	14.57	-	-	-	-

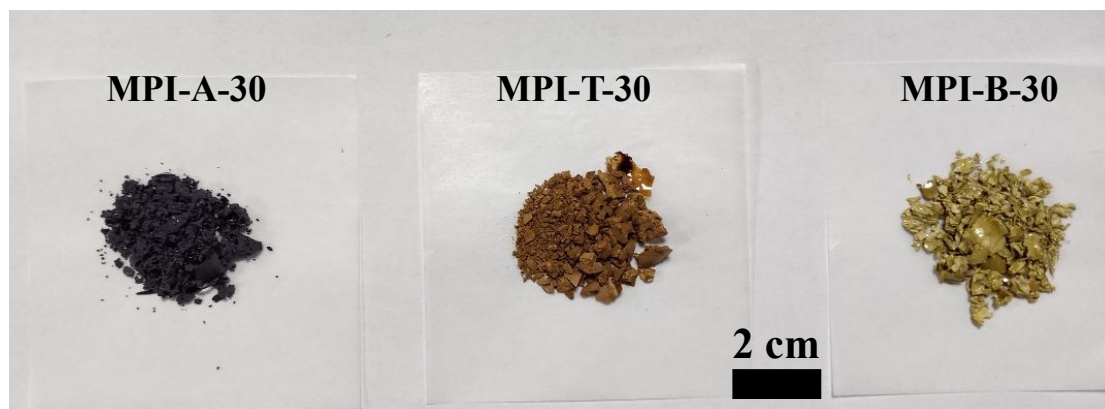


Figure S1. Digital images of as-prepared MPI-A-30, MPI-T-30 and MPI-B-30.

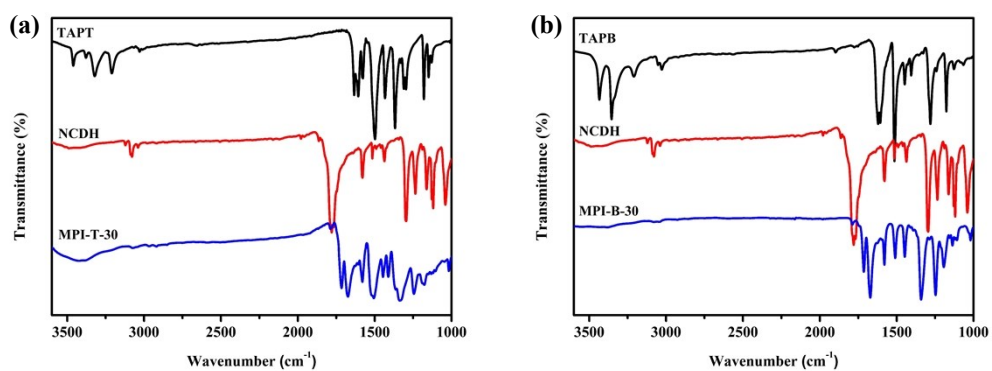


Figure S2. The FITR spectra of TAPT, NCDH and MPI-A-30 (a), as well as TAPB and MPI-B-30 (b).

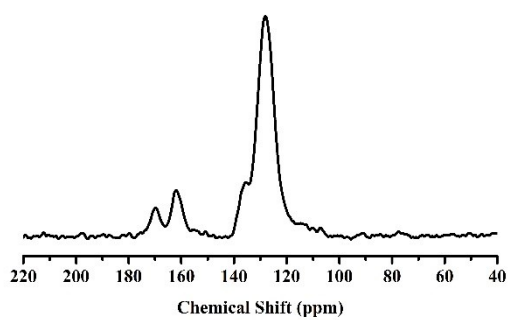


Figure S3. Solid state  $^{13}\text{C}$  cross-polarization magic-angle spinning (CP/MAS) NMR spectra of MPI-T-30.

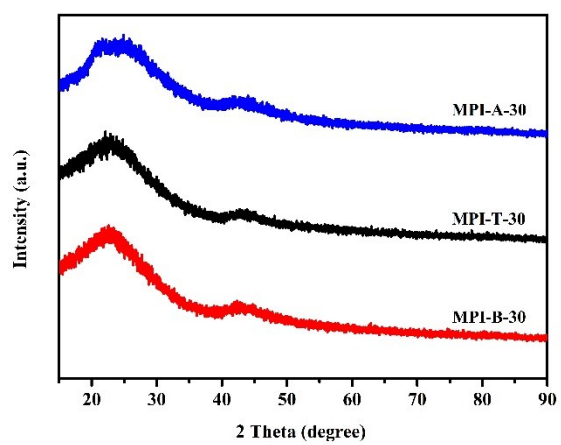


Figure S4. X-ray diffraction spectra of MPI-A-30, MPI-T-30 and MPI-B-30.



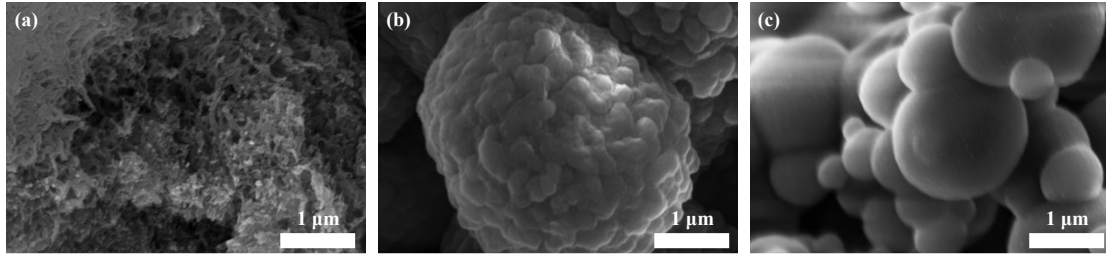


Figure S5. SEM images of MPI-A-30 (a), MPI-T-30 (b) and MPI-B-30 (c).

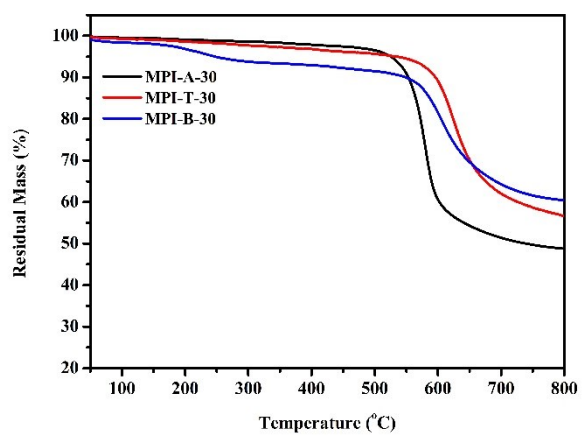


Figure S6. TGA curves of MPI-A-30, MPI-T-30 and MPI-B-30.

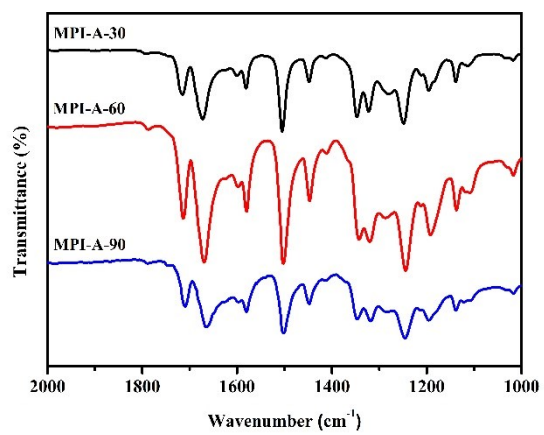


Figure S7. The FTIR spectra of MPI-A-30, MPI-A-60 and MPI-A-90.

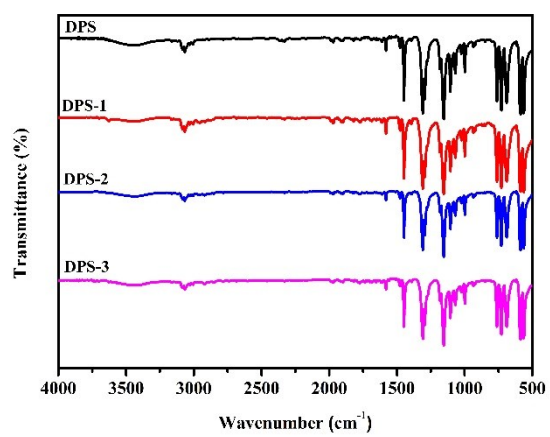


Figure S8. FTIR spectra of pure DPS and DPS-m (m represents the number of cycles).

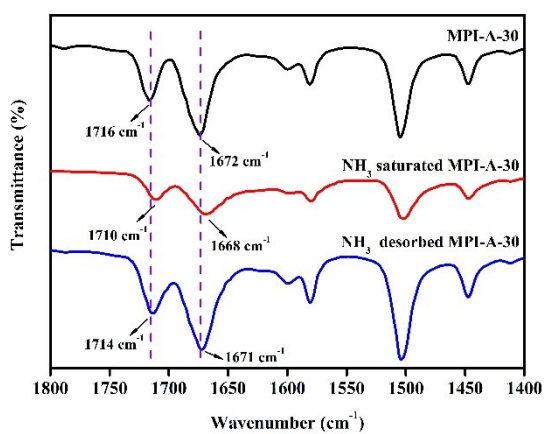


Figure S9. The FTIR spectra of MPI-A-30, NH<sub>3</sub> saturated MPI-A-30 and NH<sub>3</sub> desorbed MPI-A-30.

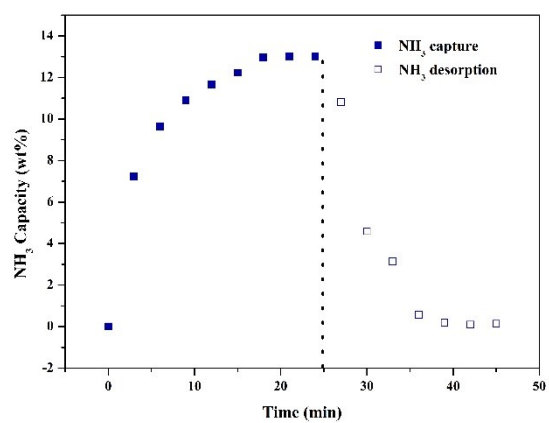


Figure S10. NH<sub>3</sub> adsorption and desorption curves of activated carbon.

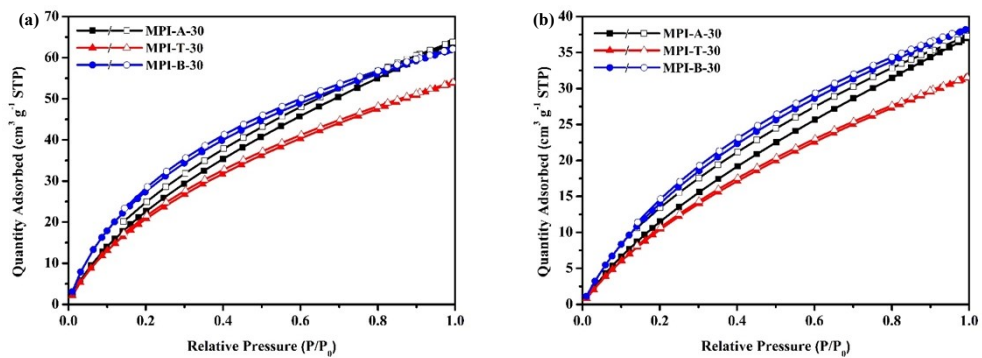


Figure S11. CO<sub>2</sub> adsorption-desorption isotherms of MPIs at 273 K (a) and 298 K (b).

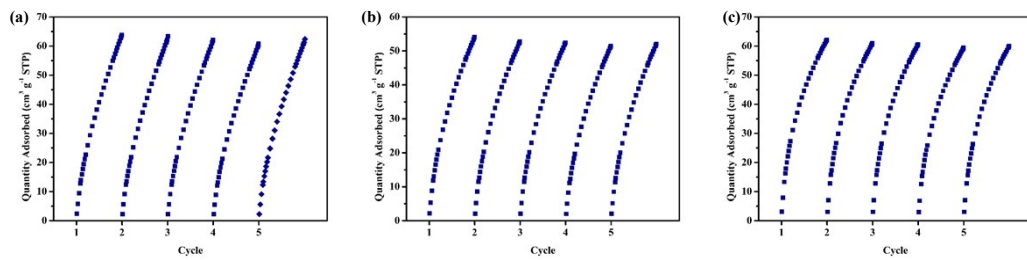


Figure S12. Five cycles of CO<sub>2</sub> adsorption at 237 K for MPI-A-30 (a), MPI-T-30 (b) and MPI-B-30 (c).



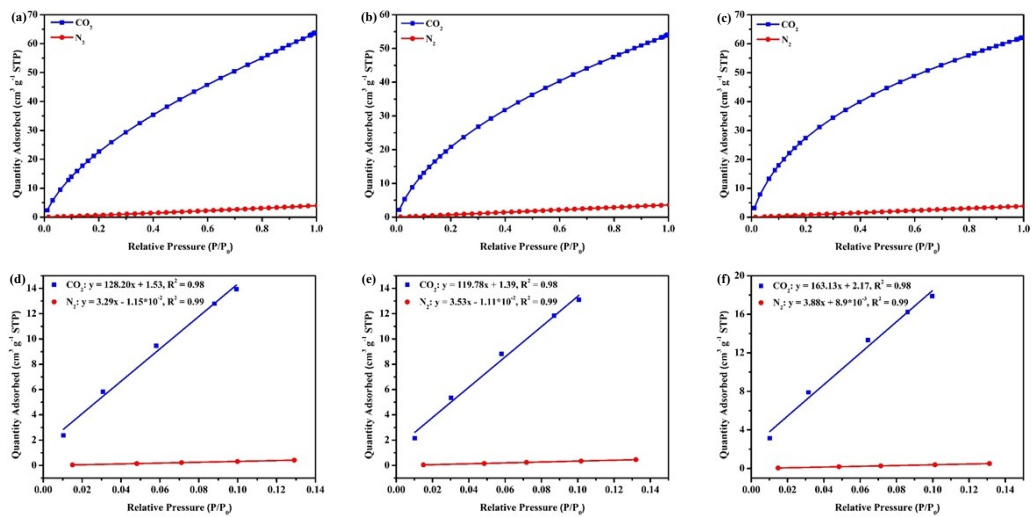


Figure S13. CO<sub>2</sub> and N<sub>2</sub> adsorption isotherms at 273 K for MPI-A-30 (a), MPI-T-30 (b) and MPI-B-30 (c). CO<sub>2</sub>/N<sub>2</sub> selectivities of MPI-A-30 (d), MPI-T-30 (e) and MPI-B-30 (f).

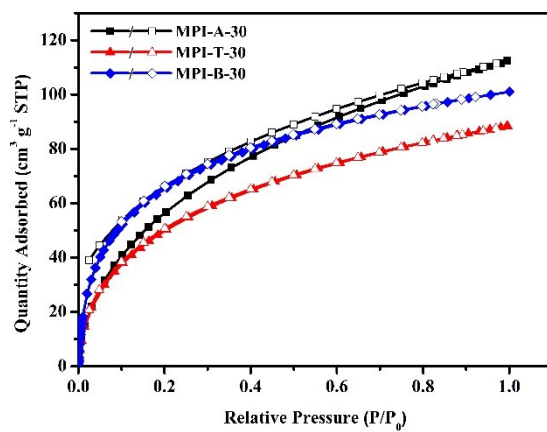


Figure S14. H<sub>2</sub> adsorption isotherms of MPI-A-30, MPI-T-30 and MPI-B-30.

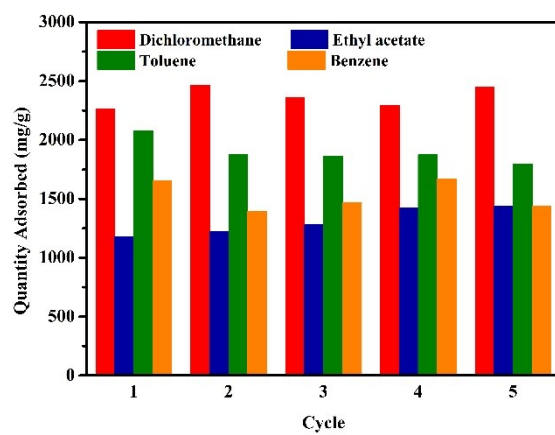


Figure S15. Volatile organic compound (VOC) uptake of MPI-A-30 at room temperature and relative saturation pressure.